



An optimal wavelet-based multi-modality medical image fusion approach based on modified central force optimization and histogram matching

Heba M. El-Hoseny¹ · Zeinab Z. El Kareh² · Wael A. Mohamed¹ · Ghada M. El Banby² · Korany R. Mahmoud³ · Osama S. Faragallah^{4,5} · S. El-Rabaie⁶ · Essam El-Madbouly² · Fathi E. Abd El-Samie⁶

Received: 7 April 2018 / Revised: 9 March 2019 / Accepted: 28 March 2019 /

Published online: 10 June 2019

© Springer Science+Business Media, LLC, part of Springer Nature 2019

Abstract

This paper introduces an optimal solution for wavelet-based medical image fusion using different wavelet families and Principal Component Analysis (PCA) based on the Modified Central Force Optimization (MCFO) technique. The main motivation of this work is to increase the quality of medical fused images in order to provide correct diagnosis of diseases for the objective of optimal therapy. This can be achieved by fusing medical images of different modalities using an optimization technique based on the MCFO. The MCFO technique gives the optimum gain parameters that achieve the best fused image quality. Histogram matching is applied to improve the overall values of the Peak Signal-to-Noise Ratio (PSNR), entropy, local contrast, and quality of the fused image. A comparative study is performed between the proposed algorithm, the traditional Discrete Wavelet Transform (DWT), and the PCA fusion using maximum fusion rule. The proposed algorithm is evaluated subjectively and objectively with different fusion quality metrics. Simulation results demonstrate that the proposed MCFO optimized wavelet-based fusion algorithm using Haar wavelet and histogram matching achieves a superior performance with the highest image quality and clearest image details in a very short processing time.

Keywords Image fusion · Discrete wavelet transform (DWT) · Modified central force optimization (MCFO) · Histogram matching

1 Introduction

Recently, the advances in the medical field and medical imaging have proved the importance of medical images as an effective tool in diagnosis of diseases. As with the great scientific

✉ Zeinab Z. El Kareh
zeinabelkareh@gmail.com

progress in imaging, it is not acceptable for technicians to depend only on their sense in detection and diagnosis of diseases [5]. Different modalities of medical images can be acquired based on different strategies. Medical images include Magnetic Resonance Images (MRI), Computed Tomography (CT) images, Positron Emission Tomography (PET) images and X-ray images. Each modality has its own benefits and limitations. Hence, integrating and merging information from two different image modalities will give fused images that are rich in details for better diagnosis [8].

Efficient image fusion methods have been implemented and applied to achieve robust fusion results. Among the broad range of image fusion methods is the DWT. The main advantages of the DWT are the minimum spectral distortion and the high Signal-to-Noise Ratio (SNR) introduced in the fused image. Unfortunately, it has some disadvantages that produce poor fusion results such as the poor treatment to long curved edges, the poor directionality, the sensitivity to shifts, the loss of phase information, and the less spatial resolution [2, 9, 23, 26, 29]. Another common method for image fusion is the PCA fusion [24, 28]. The PCA depends on decomposing the images to be fused into principle components and merging these principle components with a certain fusion rule.

Recently, optimization has captured interest of researchers to enhance the performance of several algorithms. The optimization techniques provide the optimal parameter values for an algorithm to achieve the best possible performance. Efficient optimization techniques such as Gray Wolf Optimization (GWO), CFO, and Particle Swarm Optimization (PSO), have been introduced into the field of medical image fusion, and they greatly improved the performance of the fusion techniques [3, 4, 21]. The major objective of optimization is to give clear features that can help in identifying complex activities in medical images, which is a vital task that has been considered by several authors [12, 19, 20]. Fusion techniques have also been extended to different fields other than the medical field. The fields include biometric applications, industrial applications, security applications, and satellite applications [13–17], and this in turn requires the development of efficient optimization tools for each application.

In this paper, an optimal medical image fusion technique based on DWT and MCFO for selecting the best gain parameters of the fusion process of multi-modality images is proposed. The proposed algorithm implements histogram matching to overcome the contrast limitations of the images to be fused and increase details of the fusion results. The effect of histogram matching on the fused image quality is investigated.

The rest of the paper is organized as follows. Section II introduces the algorithms of DWT and PCA fusion. Section III presents the MCFO technique. Section IV presents the proposed algorithm. Section V presents the datasets used and the computer specifications implemented. Section VI gives a discussion of the image quality metrics used to evaluate the proposed algorithm. Section VII gives the simulation results and discussions. Section VIII gives a discussion of the effect of histogram matching on the performance of the proposed fusion algorithm with optimal gain parameters. Finally, section IX presents the main conclusions.

2 Image fusion methods

Different methodologies have been introduced and studied to perform image fusion and information integration ranging from spatial-domain to transform-domain methodologies [25].

2.1 Discrete Wavelet transform (DWT) fusion

The wavelet transform is used in image processing due to its ability to preserve time- and frequency-domain details of images. Wavelets have multi-scale and multi-resolution properties, which preserve these details [31]. Wavelet fusion requires the implementation of the DWT on the images to be fused and the application of an appropriate fusion rule such as the average fusion rule or the maximum fusion rule. The DWT is implemented on the images row-by-row and then column-by-column. So, the heart of the 2D DWT is the 1D DWT. To understand the 1D DWT process, let us see Figs. 1, 2, and 3 which illustrate the wavelet decomposition filter bank, and the wavelet reconstruction filter bank as well.

The wavelet decomposition is performed with two causal filter: a low-pass filter (H_0), and a high-pass filter (H_1). On the other hand, the wavelet reconstruction is performed with two non-causal filters: G_0 , and G_1 . There is a need to achieve the Perfect Reconstruction (PR) condition [10].

To have $x_0(n)$ passed through the down-sampling and up-sampling stages, it gets multiplied by $\frac{1}{2}(1 + (-1)^n)$. Hence $X_0(z)$ is converted to $\{X_0(z) + X_0(-z)\}$. Similarly, $X_1(z)$ is converted to $\frac{1}{2}\{X_1(z) + X_1(-z)\}$.

Thus, the equation of $Y(z)$ is represented by:

$$\begin{aligned} Y(z) &= \frac{1}{2}\{X_0(z) + X_0(-z)\}G_0(z) + \frac{1}{2}\{X_1(z) + X_1(-z)\}G_1(z) \\ &= \frac{1}{2}X(z)\{H_0(z)G_0(z) + H_1(z)G_1(z)\} + \frac{1}{2}X(-z)\{H_0(-z)G_0(z) + H_1(-z)G_1(z)\} \end{aligned} \quad (1)$$

For aliasing cancellation, the coefficient of $X(-z)$ needs to be cancelled out. Hence, $\{H_0(-z)G_0(z) + H_1(-z)G_1(z)\} = 0$. This can be achieved if:

$$H_1(z) = z^{-k}G_0(-z) \text{ and } G_1(z) = z^kH_0(-z) \quad (2)$$

where k must be odd (usually $k = \pm 1$).

The second PR condition is:

$$\{H_0(z)G_0(z) + H_1(z)G_1(z)\} = 2 \quad (3)$$

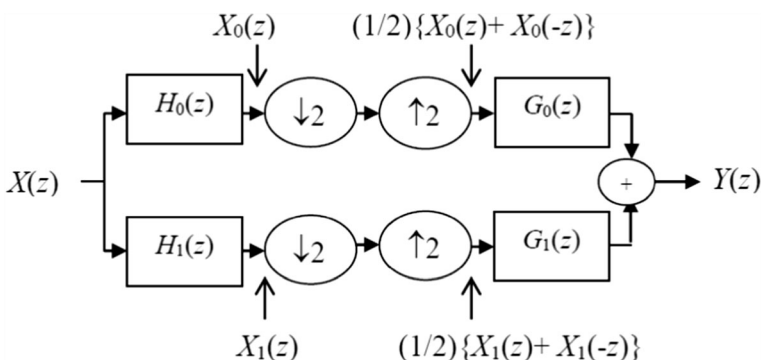


Fig. 1 Two-channel filter bank of the DWT

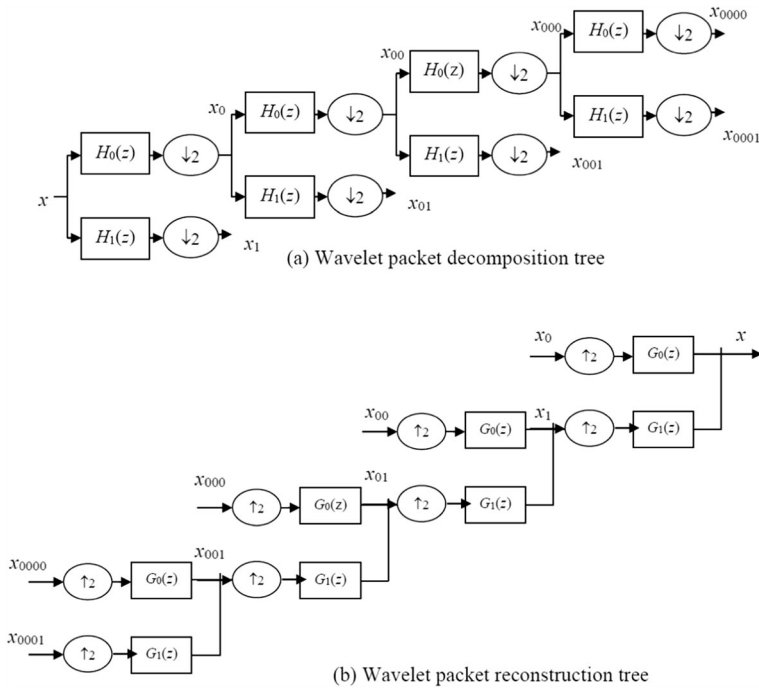


Fig. 2 The filter bank structure of wavelet-based decomposition and reconstruction

We can define $P(z) = H_0(z)G_0(z)$ and substitute from Eq. (2) into Eq. (3), then the equation becomes:

$$H_0(z)G_0(z) + H_1(z)G_1(z) = P(z) + P(-z) = 2 \quad (4)$$

To satisfy Eq. (4), all odd powers of z in $P(z)$ need to cancel with those of $P(-z)$. This can be achieved only if:

$$P(z) = \cdots + p_5 z^5 + p_3 z^3 + p_1 z + 1 + p_1 z^{-1} + p_3 z^{-3} + p_5 z^{-5} + \cdots \quad (5)$$

To summarize the design steps of the PR filters:

- 1- Choose the polynomial $P(z)$ to be a zero-phase polynomial.

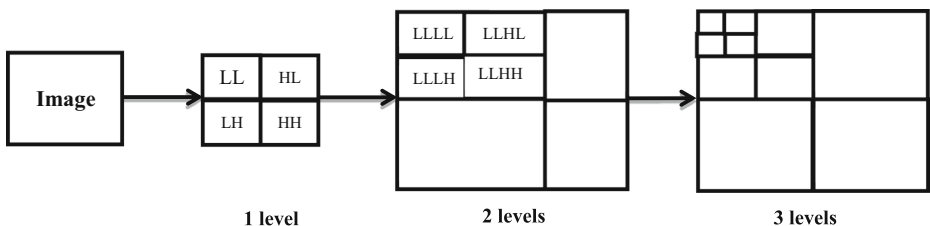


Fig. 3 Image decomposition scheme using 2D DWT

- 2- Factorize $P(z)$ into $H_0(z)$ and $G_0(z)$ with similar lowpass frequency responses.
- 3- Calculate $H_1(z)$ and $G_1(z)$ from $H_0(z)$ and $G_0(z)$.

To simplify the steps, we can use the following relation:

$$P(z) = P_t(Z) = 1 + p_{t,1}Z + p_{t,3}Z^3 + p_{t,5}Z^5 + \cdots \quad (6)$$

where

$$Z = \frac{1}{2}(z + z^{-1}) \quad (7)$$

The fusion process of MR and CT images is performed with a fusion rule, which may be application dependent or not, and it can also be dependent on the sub-band of interest or not. The fusion rule used may be the minimum fusion rule, maximum fusion rule, weighted average rule, or average fusion rule. Generally, the fusion of two images using DWT is illustrated in Fig. 4.

To obtain the wavelet coefficients, four orthogonal wavelet families are considered in this paper: Haar, Daubechies, Coiflet, and Discrete approximation of the Meyer wavelets [11, 18]. These wavelet families are implemented and compared to determine which one has the best performance with the proposed algorithm. The main differences between these families are shown in Fig. 5.

2.2 Principal component Analysis (PCA) fusion

One of the most popular image fusion approaches is based on PCA. It can be applied using three different methods: calculating eigenvalues and eigenvectors, Singular Value Decomposition (SVD), or estimating co-variance matrix. The first method depends on calculating eigenvalues and eigenvectors. It achieves high quality factors in the fused image, but causes some sort of blurring of the output image. The second method depends on the SVD, and this method produces a better fused image, however, it has some delay, which becomes longer with larger image sizes (in pixels). The third method depends on estimating a co-variance matrix, and it produces a convenient, more clear, and informative image. This method is adopted in this paper. The weights for each input image are determined in this method using the eigenvector corresponding to the largest eigenvalue of the co-variance matrix of each source image [1].

We can summarize the fusion steps as follows [29]:

- (1) Produce column vectors from the input images.

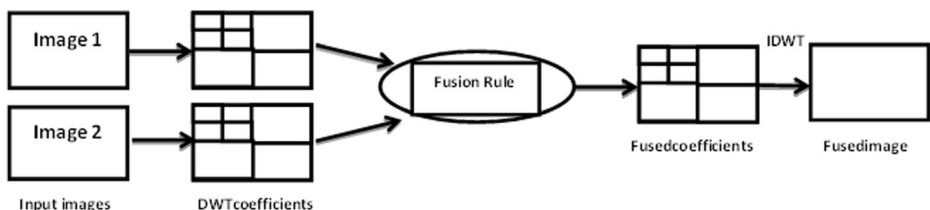


Fig. 4 General fusion process with DWT

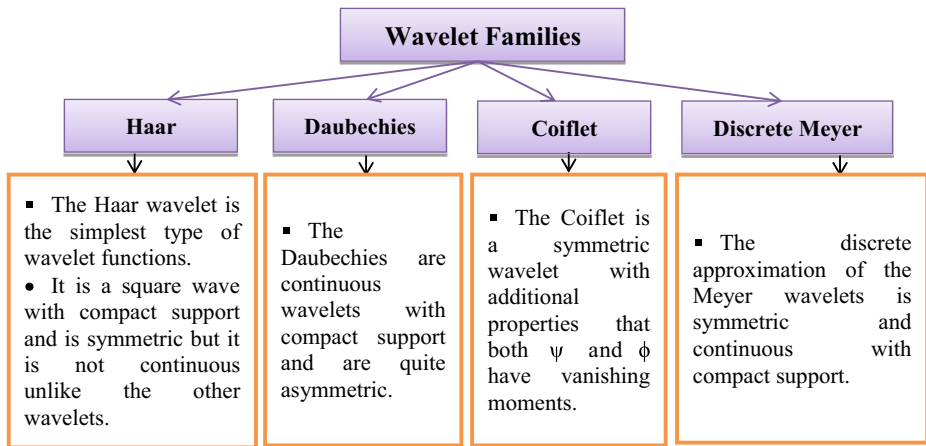


Fig. 5 Different wavelet families of DWT

- (2) Calculate the co-variance matrix of the two column vectors in step 1 by the following equation:

$$\text{Covariance } (X.Y) = \frac{\sum_{i=1}^n (X_i - \bar{X})(Y_i - \bar{Y})}{(n-1)} \quad (8)$$

where \bar{X} and \bar{Y} are the mean values of the images X and Y .

- (3) Calculate the eigen vector corresponding to the largest eigen value of the co-variance matrix.

For a $C_{p \times p}$ covariance matrix, the scalar values λ_p are the eigen values of C such that,

$$C U_p = \lambda_p U_p \quad (9)$$

where U_p is the eigen vector corresponding to the eigen value λ_p .

- (4) Compute the eigen values λ_p of C , where $\lambda_1 > \lambda_2 > \dots > \lambda_p$, from the relation below:

$$|C - \lambda_p I| = 0 \quad (10)$$

- (5) Normalize eigen vectors to get the weight values to multiply them with each pixel of the two input images.
- (6) Fuse the two scaled matrices to produce the fused image matrix as follows:

$$I_{\text{fused}} = P(1)I_1 + P(2)I_2 \quad (11)$$

where I and I are the two input images and $P(1)$ and $P(2)$ are the weights of the selected eigen vectors.

3 Image registration

It is necessary to perform an image registration step between images with different modalities to guarantee coordinate alignment. Among different methods used to perform image registration is the intensity-based method, which is adopted in this paper [30]. The frame work describes the intensity-based registration method applied to the two misaligned images is shown in Fig. 6. The following steps summarize the applied registration process:

1. Application of resampling rigid, affine, or similarity transformation on the misaligned image.

$$\text{Rigid Transform } T_{\mu}(\mathbf{x}) = \mathbf{R}(\mathbf{x}-c) + t + c \quad (12)$$

$$\text{Similarity } T_{\mu}(\mathbf{x}) = s\mathbf{R}(\mathbf{x}-c) + t + c \quad (13)$$

$$\text{Affine } T_{\mu}(\mathbf{x}) = \mathbf{A}(\mathbf{x}-c) + t + c \quad (14)$$

where $T_{\mu}(\mathbf{x})$ is the transform; t is the translation; c is a constant; s is the similarity, \mathbf{R} is the rotational matrix, and \mathbf{A} is a matrix without restrictions.

2. Similarity evaluation with the reference image.

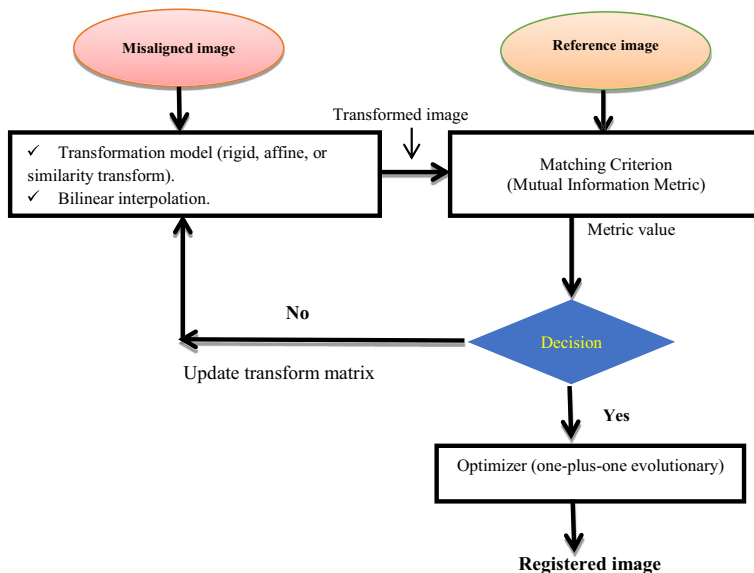


Fig. 6 Intensity-based image registration framework

3. Optimization of the transformation applied on the misaligned image based on the similarity metric value.
4. Evaluation of registration accuracy based on the similarity metric value without the need for definition of landmarks or features.

4 The modified central force optimization (MCFO)

The CFO is a new optimization approach presented to solve many practical problems by using Newton's relations for moving objects under the effect of gravity [3]. The optimization process is performed like any optimization technique starting with parameters initialization followed by computing probe position and acceleration. The MCFO is implemented to increase the optimization accuracy and improve the capability of the memory to update the probe position as shown in the following equations:

The updated acceleration:

$$A_{j-1}^p = G_j \sum_{\substack{k=1 \\ k \neq p}}^{N_p} U(M_{j-1}^k - M_{j-1}^p) \times (M_{j-1}^k - M_{j-1}^p) \frac{\alpha (R_{j-1}^k - R_{j-1}^p)}{\|R_{j-1}^k - R_{j-1}^p\|} \quad (15)$$

$$G_j = G_0 \exp\left(\frac{-j\gamma}{N_t}\right) \quad (16)$$

The updated probe position:

$$R_j^p = R_{j-1}^p + C1_j rand_1 A_{j-1}^p \Delta t^2 + C2_j rand_2 (R_{best} - R_{j-1}^p) \Delta t, \quad j \geq 1 \quad (17)$$

$$C1_j = C1^{max} - \frac{C1^{max} - C1^{min}}{N_t} \times j \quad (18)$$

$$C2_j = C2^{min} + \frac{C2^{max} - C2^{min}}{N_t} \times j \quad (19)$$

where G_j is the value of the current gravitational constant, G_0 is the initial gravitational constant, γ is the descending coefficient factor, p is the probe number, N_t is the maximum number of iterations, $C1$ and $C2$ are the time-varying acceleration coefficients, $rand_1$ and $rand_2$ are two random numbers in the range of $[0, 1]$, $U(\cdot)$ is the unit step function, α and β are the CFO exponents, and Δt is taken as a unit time step increment.

For the proposed algorithm, the fitness value can be the maximum local contrast, entropy, or PSNR of the fused images at different gain parameters as they are the most commonly used and trusted metrics for evaluating the image quality. The gain parameter values a_1 , b_1 of high-frequency sub-bands and a_2 , b_2 of low-frequency sub-bands are constrained to values in the interval $[0, 1]$, $a_1 + b_1 = 1$, and $a_2 + b_2 = 1$.

5 The proposed MCFO optimized wavelet-based fusion algorithm

Optimization has become a very important trend for developing the performance of many traditional techniques by providing the optimum parameters that enhance the performance of these techniques easily in few seconds. In medical image fusion, DWT is a very common and widely-used algorithm that minimizes the spectral distortion and increases the PSNR. On the other hand, PCA is a simple fusion algorithm. We here introduce a new technique to improve their performance, and obtain higher image quality, and better visualization based on MCFO optimization and adaptive histogram equalization.

The proposed MCFO optimized wavelet-based fusion technique is illustrated in the following steps:

- 1) First the multi-modality images are resized and registered using the intensity-based image registration technique as discussed in section IV.
- 2) The different wavelet filters of the DWT (Haar, db1, Coiflet 1, or discrete Meyer) are implemented to obtain the DWT coefficients of both images as illustrated in section III.
- 3) The MCFO optimization technique is used to generate and update gain parameter values in order to obtain the best set of gain parameters, section V.
- 4) The weighted average fusion rule is applied on the obtained DWT coefficients according to the following equation:

$$F = G_1.I_1 + G_2.I_2 \quad (20)$$

where F is the fused image, I_1 and I_2 are the input images, and G_1 and G_2 are the gain parameters.

- 5) The inverse DWT is computed on the fused coefficients to get the pre-fused image which is evaluated according to the highest local contrast, highest PSNR, and highest entropy to determine the optimum set of gain parameters.
- 6) For more enhancement of the optimum fused image, adaptive histogram equalization is applied on the final fusion process.

The proposed approach is illustrated in the block diagram shown in Fig. 7.

6 Datasets and computer specifications

Simulation results were evaluated using MATLAB R2015a with windows 7 on an Intel laptop with core i3 processor, and 3.0 GB RAM. The proposed MCFO optimized wavelet-based fusion algorithm was implemented on four different datasets of different modalities. The first dataset introduces Alzheimer disease for 71 years old man including MRI modality that represents the physical change and the effect of the disease on the anatomical structure of the brain and PET modality that represents the brain functionality for Alzheimer patient. The second dataset introduces Thymic

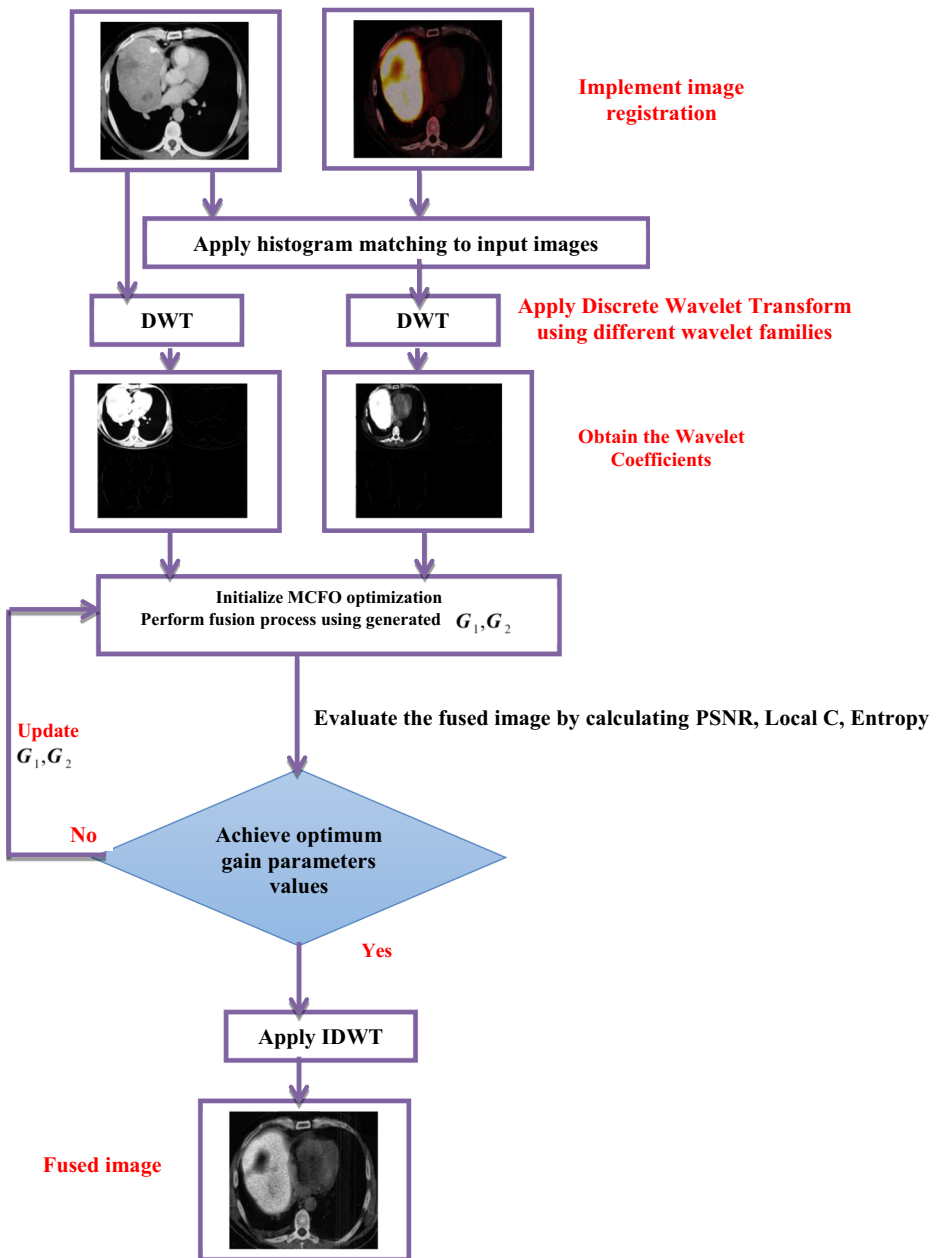


Fig. 7 The block diagram of the proposed MCFO optimized wavelet-based fusion system

Neuroendocrine Carcinoma disease for 47 years old man including CT and PET images. The third and fourth datasets introduce a brain tumor with MRI and CT images (<https://medpix.nlm.nih.gov/home>. Last access 10/7/2017). These datasets are shown in Fig. 8.

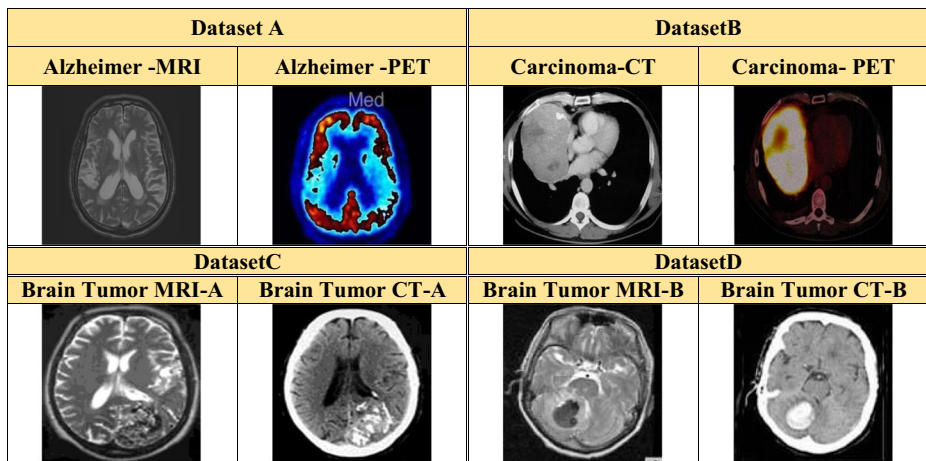


Fig. 8 The implemented datasets for Alzheimer, Thymic Neuroendocrine Carcinoma, and brain tumor cases

7 Evaluation metrics

The comparative analysis and performance evaluation of the proposed multi-modality medical image fusion system are performed, objectively and subjectively. Different metrics are used to evaluate the proposed algorithm such as average gradient, local contrast, standard deviation, edge intensity, entropy, PSNR, and Q^{ab}/f [7, 27].

1) Average Gradient (AVG)

The average gradient represents the details contrast and the amount of texture variation in the image. It is calculated as:

$$g = \frac{1}{(M-1)(N-1)} \sum_{i=1}^{(M-1)(N-1)} \sqrt{\frac{\left(\frac{\partial f}{\partial x}\right)^2 + \left(\frac{\partial f}{\partial y}\right)^2}{2}} \quad (21)$$

where M and N are the image dimensions.

2) Local Contrast (local C)

It is an index for the image quality and purity of view. It is calculated using the equation:

$$C_{local} = \frac{|\mu_{target} - \mu_{background}|}{\mu_{target} + \mu_{background}} \quad (22)$$

where μ_{target} is the mean gray-level of the target image in the local region of interest, and $\mu_{background}$ is the mean of the background in the same region. The larger value of C indicates more purity of the image.

3) Standard Deviation (STD)

It is used to determine how much variation of the data is from the average or mean value. The image is said to be clearer if its STD value is larger. The STD is calculated using the equation:

$$STD = \sqrt{\frac{\sum_{i=1}^M \sum_{j=1}^N |f(i,j) - \mu|^2}{MN}} \quad (23)$$

where M and N represent the dimensions of the image $f(i,j)$, and the mean value is represented by μ .

4) Edge Intensity (S)

A higher edge intensity of an image represents a higher image quality and more clearness. Edge intensity of the image f can be measured using Sobel operator (S).

$$s_x = f * h_x, \quad s_y = f * h_y \quad (24)$$

$$\text{where } h_x = \begin{pmatrix} 1 & 0 & 1 \\ -2 & 0 & 2 \\ -1 & 0 & 1 \end{pmatrix}, h_y = \begin{pmatrix} -1 & -2 & -1 \\ 0 & 0 & 0 \\ 1 & 2 & 1 \end{pmatrix} \quad (25)$$

$$S = \sqrt{(s_x^2 + s_y^2)}$$

5) Image Entropy (E)

It is a measure of the amount of information contained in the image. If the probability density p is known, then the image information content can be estimated regardless of its interpretation using entropy E , and it can be defined as:

$$E = -\sum_{i=0}^n p(x_i) \log p(x_i) \quad (26)$$

where x_i of the i^{th} point is its gray-scale value, and p is its probability. It is said that the image is better if it has a large value of E .

6) Peak Signal-to-Noise Ratio (PSNR)

It is a quantitative measure based on the Root Mean Square Error (RMSE), and it is calculated as:

$$PSNR = 10 \times \log \left(\frac{(f_{max})^2}{RMSE^2} \right) \quad (27)$$

where f_{max} represents the maximum pixel gray level value in the reconstructed image.

7) Xydeas and Petrovic Metric ($Q^{ab/f}$)

This metric is used to measure the transferred edge information from source images to the fused one. A normalized weighted version of that metric can be calculated as follows:

$$Q^{AB/F} = \frac{\sum_{m=1}^M \sum_{n=1}^N \left(Q_{(m,n)}^{AF} W_{(m,n)}^{AF} + Q_{(m,n)}^{BF} W_{(m,n)}^{BF} \right)}{\sum_{m=1}^M \sum_{n=1}^N W_{(m,n)}^{AF} + W_{(m,n)}^{BF}} \quad (28)$$

where $Q_{(m,n)}^{AF}$, $Q_{(m,n)}^{BF}$ are the edge information preservation values, and $W_{(m,n)}^{AF}$, $W_{(m,n)}^{BF}$ are their weights.

8 Results and discussions

The registration of input images is the first and the most important pre-processing step in the proposed MCFO-optimized wavelet-based fusion algorithm. It confirms the size matching, orientation matching, and the same alignment boundaries of the input dataset images. This provides better information fusion with large detail information and image quality [22]. The registration process of input images is clarified in Fig. 9.

Figure 9 introduces the registration process of the input datasets (Alzheimer, Thymic Neuroendocrine Carcinoma, and Brain tumor cases A and B). Figure 9 (a, b, and c) show the original unregistered images of the input datasets. It is obvious that input images are not aligned to each other and this can produce artifacts in the fused images and decrease the efficiency of the proposed algorithm. Therefore, the registration is necessary. Assume that the Alzheimer -MRI, Carcinoma-CT, and Brain Tumor MRI-A and B are the target images and Alzheimer -PET, Carcinoma- PET, and Brain Tumor CT-A and B are the images to be registered. Fig. 9(d) presents the obtained registered images using the intensity-based image registration. Figure 9 (e) proves a good matching between input images to be suitable for the fusion process.

In the proposed MCFO-optimized wavelet-based fusion algorithm, the best gain parameters obtained are used for fusing the coefficients of the DWT of different wavelet filters. The MCFO optimization technique is also applied to the PCA fusion technique. Finally, a post-processing step for enhancing the local contrast using the adaptive histogram equalization is implemented. The proposed algorithms are evaluated and compared to the traditional DWT and PCA using maximum fusion rule to study the effectiveness of the MCFO optimization technique. The performance evaluation of the proposed algorithms and simulation results with different datasets are illustrated in Tables (1, 2, 3, and 4).

These results can be represented by the charts in Figs. (10 and 11) proving the great improvement caused by of the proposed MCFO-optimized wavelet-based fusion algorithm using Haar filter in values of average gradient, local contrast, standard deviation, and edge intensity. This makes the proposed algorithm provide better fused images with much more detailed information and clear edges for an accurate diagnosis.

The general concept in evaluating the performance of a fusion algorithm is that it does not depend only on one or two definite metrics. There is a combination of the evaluation

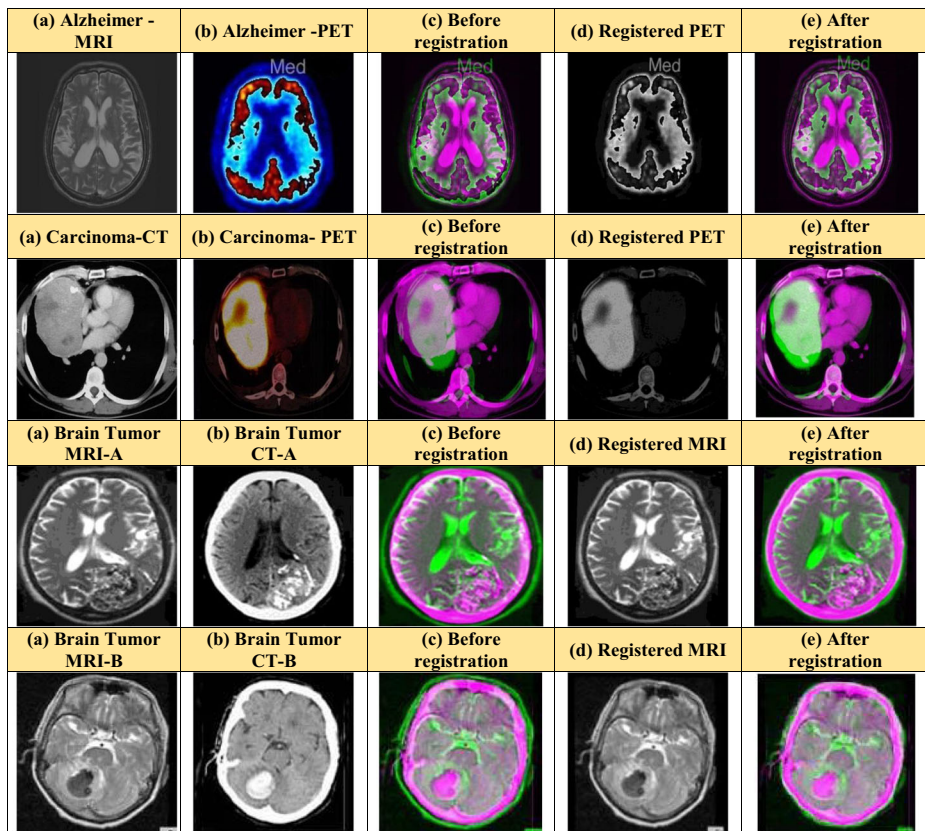


Fig. 9 Registration process of input datasets (Alzheimer, Thymic Neuroendocrine Carcinoma, and Brain tumor cases)

metrics that prove a higher image quality and better visualization. Hence, many metrics have been tested for the proposed algorithms. From Tables (1, 2, 3, and 4), it can be seen that the optimization solutions for gain parameters using MCFO optimization technique

Table 1 Simulation results of the proposed algorithm with optimum gain parameters according to local C, PSNR, and entropy with different wavelet filters (Haar – db1- Coif 1- discrete meyer) compared to traditional DWT and PCA with maximum fusion rule on dataset A

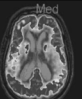
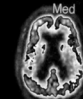
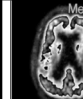
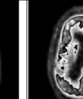
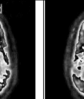
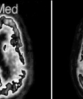
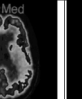


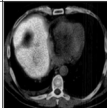
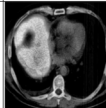
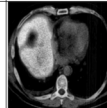
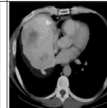

Alzheimer 512 * 512	Haar - Max fuion rule	OPT-Haar 0.9706 0.0294	OPT-db1 0.9826 0.0174	OPT-Coif1 0.9208 0.0792	OPT-dmey 0.9833 0.0167	PCA- Max fuion rule [2]	OPT-PCA 0.0021 0.9979
AVG	0.0141	4.9447	0.0192	0.0191	0.0192	0.0111	0.0174
Local C	0.4083	0.6740	0.6771	0.6577	0.6773	0.5348	0.6861
STD 2	0.1728	66.0347	0.2606	0.2557	0.2606	0.1738	0.2410
Edge I	0.1482	52.7522	0.2055	0.2034	0.2055	0.1199	0.1863
Entropy	5.3675	6.4468	6.1847	6.2848	6.1836	5.3492	5.9185
PSNR	66.9597	9.4981	67.0172	67.0254	67.0243	74.0808	69.9603
Q^{ab/f}	0.7395	0.0032	0.2004	0.2043	0.1996	0.3315	0.2813
Visual inspection							

Table 2 Simulation results of the proposed algorithm with optimum gain parameters according to local C, PSNR, and entropy with different wavelet filters (Haar – db1- Coif 1- discrete meyer) compared to traditional DWT and PCA with maximum fusion rule on dataset B

Carcinoma 512 × 512	Haar - Max fuion rule	OPT-Haar 0.9754 0.0246	OPT-db1 0.9656 0.0344	OPT- Coif1 0.9092 0.0908	OPT- dmey 0.9365 0.0635	PCA- Max fuion rule [2]	OPT-PCA 0.9888 0.0112
AVG	0.0177	4.1825	0.0163	0.0167	0.0164	0.0131	0.0234
Local C	0.4891	0.5276	0.5224	0.5077	0.5127	0.4680	0.5935
STD 2	0.2929	57.7554	0.2277	0.2334	0.2305	0.2379	0.2586
Edge I	0.1870	44.4210	0.1731	0.1776	0.1746	0.1401	0.2434
Entropy	6.7838	6.6833	6.7237	6.8425	6.7826	6.4805	6.9695
PSNR	69.8492	10.0662	65.5483	64.0013	64.7010	69.1668	70.8502
Q^{abf}	0.6529	0.0028	0.0503	0.0561	0.0563	0.1439	0.2312
Visual inspection							

have improved the performance of the traditional fusion techniques of DWT with different wavelet filters and PCA with maximum fusion rule. This result can be confirmed for different datasets of different diseases used with the proposed algorithm. In particular, the proposed MCFO-optimized wavelet-based fusion algorithm using Haar wavelet filter has a more superior performance than those of the other wavelet filters and optimum PCA with the highest values of average gradient, local contrast, standard deviation, and edge intensity. This provides higher detailed information, higher edge clearness, and better detailed contrast. On the other hand, the values of PSNR and quality factor have been decreased, because the fusion process produces a new image of new characteristics different from the input images. So, the transferred edge information from input images to the fused images represented by quality factor has been decreased.

8.1 Memory computational complexity and processing time

To test the applicability of the proposed fusion algorithm and its efficiency, two factors based on memory size and processing time are calculated for an image of size $N \times N$ compared with some selected fusion methods. Table 5 ensures that the proposed optimized DWT can achieve less processing time with less memory size compared to other methods like curvelet, AWT and

Table 3 Simulation results of the proposed algorithm with optimum gain parameters according to local C, PSNR, and entropy with different wavelet filters (Haar – db1- Coif 1- discrete meyer) compared to traditional DWT and PCA with maximum fusion rule on dataset C


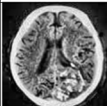
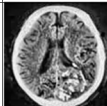
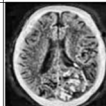
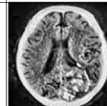
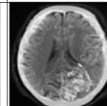
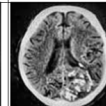
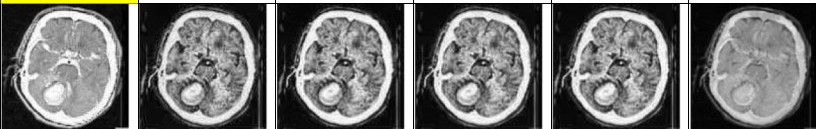
Brain tumor A 128 × 128	Haar - Max fuion rule	OPT-Haar 0.9916 0.0084	OPT-db1 0.9651 0.0349	OPT- Coif1 0.8990 0.1010	OPT- dmey 0.9620 0.0380	PCA- Max [2] fuion rule	OPT-PCA 0.0388 0.9612
AVG	0.0639	18.0488	0.0700	0.0697	0.0698	0.0382	0.0615
Local C	0.7443	0.9113	0.9001	0.8852	0.8990	0.6650	0.8932
STD 2	0.2940	74.7509	0.2928	0.2832	0.2915	0.2572	0.2759
Edge I	0.6325	172.0838	0.6754	0.6776	0.6740	0.3884	0.5965
Entropy	7.7377	7.7413	7.7762	7.8046	7.7791	7.5646	7.6181
PSNR	60.6781	6.1796	66.5596	66.0643	66.5878	68.9911	67.9369
Q^{abf}	0.4746	0.0011	0.2806	0.2831	0.2834	0.2408	0.2863
Visual inspection							

Table 4 Simulation results of the proposed algorithm with optimum gain parameters according to local C, PSNR, and entropy with different wavelet filters (Haar – db1- Coif 1- discrete meyer) compared to traditional DWT and PCA with maximum fusion rule on dataset D

Brain tumor B 128 * 128	Haar - Max fuion rule	OPT-Haar 0.9413 0.0587	OPT-db1 0.9681 0.0319	OPT- Coif1 0.9404 0.0596	OPT- dmey 0.9473 0.0527	PCA- Max fuion rule [2]
AVG	0.0566	16.7590	0.0650	0.0640	0.0642	0.0330
Local C	0.7060	0.8437	0.8366	0.8308	0.8328	0.6068
STD 2	0.3358	78.0424	0.3218	0.3141	0.3154	0.2889
Edge I	0.5467	161.2350	0.6360	0.6270	0.6288	0.3340
Entropy	7.3122	7.4048	7.3760	7.5959	7.6014	7.0595
PSNR	62.7272	6.1041	67.9043	67.3093	67.4586	67.2248
Q ^{ab/f}	0.3074	5.99*10 ⁻⁴	0.2206	0.2203	0.2203	0.1849
Visual inspection						

the NSCT. It is clear from the output results in Table 5 that the proposed technique based on MCFO optimizer has a processing time of 2.64 s, which guaranetees its applicability in real time.

8.2 Histogram matching (HM)

The histogram matching is a method for enhancing the contrast of the image by transforming the histogram of one input image to match the histogram of the other input image before the fusion process. This can be used for enhancing the local contrast of the fused image and improving values of PSNR and quality factor. Matching histograms between input images can be performed according to the following equations [6]:

8.2.1 Computation of the mean values of both images as follows

$$\mu = \frac{1}{M \times N} \sum_{i=1}^M \sum_{j=1}^N f(i, j) \quad (29)$$

where M and N are the dimensions of the image.

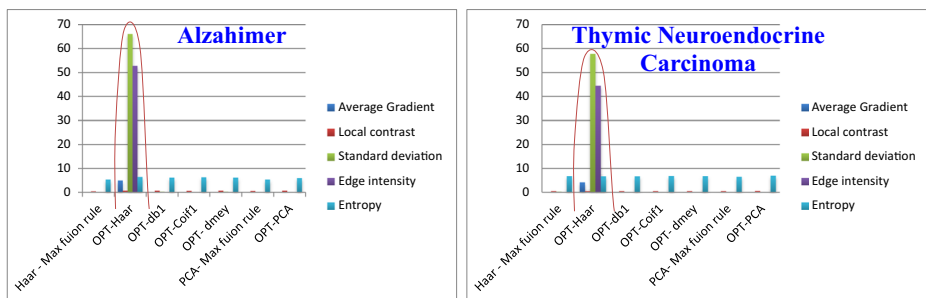


Fig. 10 Performance evaluation of the proposed MCFO-optimized wavelet-based fusion algorithm with different wavelet families and traditional DWT and PCA with maximum fusion rule on datasets A and B

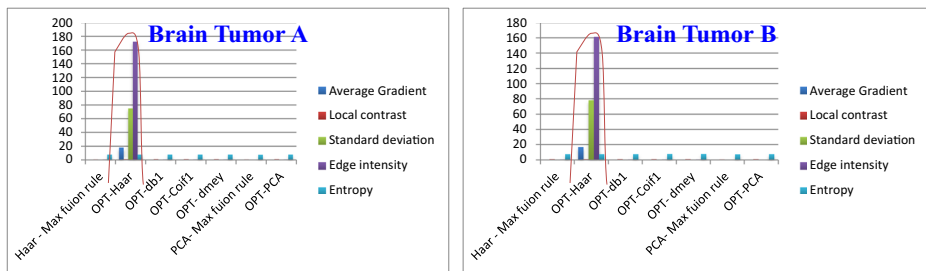


Fig. 11 Performance evaluation of the proposed MCFO-optimized wavelet-based fusion algorithm with different wavelet families and traditional DWT and PCA with maximum fusion rule on datasets C and D

8.2.2 Calculation of the standard deviation of both images as follows

$$\sigma = \sqrt{\frac{\sum_{i=1}^M \sum_{j=1}^N (f(i, j) - \mu)^2}{M \times N}} \quad (30)$$

8.2.3 Estimation of a correction factor as follows

$$c_r = \frac{\sigma_1}{\sigma_2} \quad (31)$$

where σ_1 is the standard deviation of the reference image $f_1(i, j)$, and σ_2 is the standard deviation of the image to be matched $f_2(i, j)$.

8.2.4 Estimation of a mean correction term as follows

$$M_c = \mu_1 - (c_r \times \mu_2) \quad (32)$$

where μ_1 is the mean of the reference image $f_1(i, j)$, and μ_2 is the mean of the image to be matched $f_2(i, j)$.

8.2.5 Estimation of the matched image as follows

$$f_{2\mu}(i, j) = (f_2(i, j) \times c_r) + M_c \quad (33)$$

Table 5 Memory computational complexity for the proposed DWT and the state-of-the-art fusion techniques

	PCA [2]	The proposed DWT	Curvelet [34]	NSCT [33]	Fuzzy [3]	AWT [32]
Memory cost	3 N	6 N	39 N	2 $N(I + J) + 2 N$	3 N	19 N
Processing time in sec	1.267	2.64	1252.8	103.11	10.04	1.18

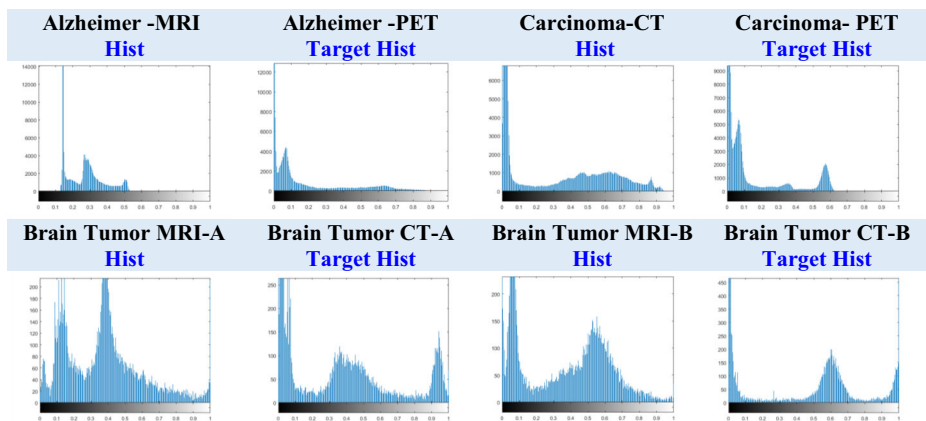


Fig. 12 The histogram of the input datasets (Alzheimer, Thymic Neuroendocrine Carcinoma, and Brain tumor cases)

Figure 12 shows the histograms of the original images of input datasets. It is obvious that some images have stretched histogram, while the others have intensity values limited to a smaller range. The main concept of histogram matching implemented in the proposed algorithm is matching images with narrow histograms to images with stretched histograms. This may increase the clearness of images and improve PSNR values.

From Tables (6 and 7), it can be seen that the histogram matching increases the PSNR and the entropy values of the proposed MCFO-optimized wavelet-based fusion algorithm using Haar wavelet filter, greatly. However, the lower values of the other quality metrics, the clearness and visualization of the fused image are much better affected by the higher values of PSNR, entropy, local contrast, and good quality factor. Hence, the proposed MCFO-optimized wavelet-based fusion algorithm using Haar wavelet filter and the histogram matching achieves a better performance providing an enhanced image quality and introduces better images helping for better diagnosis.

This can be better explained by the following chart seen in Fig. 13.

From Fig. 13, it can be noticed that the proposed MCFO-optimized wavelet-based fusion algorithm with Haar filters has lower PSNR values for all cases (Alzheimer, Thymic Neuroendocrine Carcinoma, and Brain tumor cases) compared to the other wavelet families. So, the histogram matching is applied to the proposed algorithm to improve the PSNR values, which

Table 6 Effect of using histogram matching on the proposed MCFO-optimized wavelet-based fusion algorithm using Haar wavelet filter compared to traditional DWT on datasets A and B

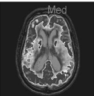
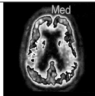
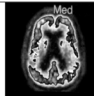

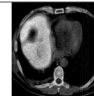
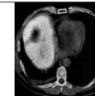


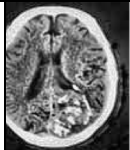

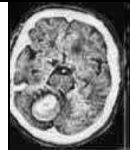
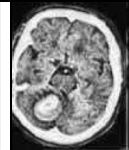
	Max Haar	OPT-Haar 0.9706 0.0294	OPT-Haar HM	Max Haar	OPT-Haar 0.9754 0.0246	OPT-Haar HM
AVG	0.0141	4.9447	0.0192	0.0177	4.1825	0.0163
Local C	0.4083	0.6740	0.6744	0.4891	0.5276	0.5264
STD 2	0.1728	66.0347	0.2600	0.2929	57.7554	0.2269
Edge I	0.1482	52.7522	0.2052	0.1870	44.4210	0.1728
Entropy	5.3675	6.4468	6.1902	6.7838	6.6833	6.6992
PSNR	66.9597	9.4981	66.9950	69.8492	10.0662	65.8493
Q^{ab/f}	0.7395	0.0032	0.2003	0.6529	0.0028	0.0485
Visual inspection						

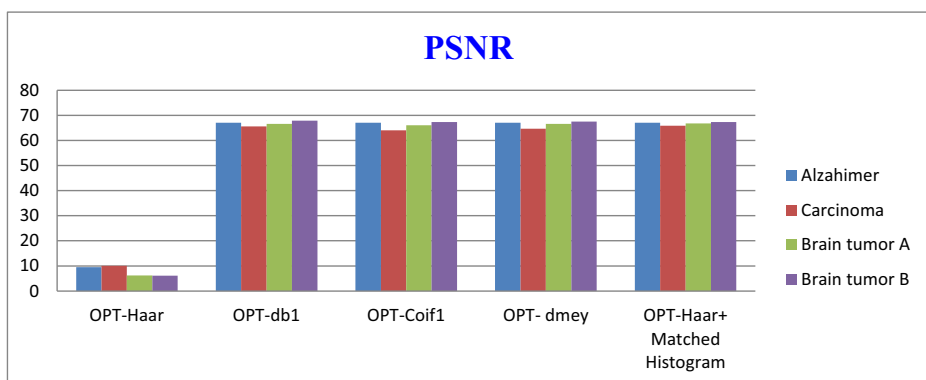
Table 7 Effect of using histogram matching on the proposed MCFO-optimized wavelet-based fusion algorithm using Haar wavelet filter compared to traditional DWT on datasets C and D

	Max Haar	OPT-Haar 0.9916 0.0084	OPT-Haar HM	Max Haar	OPT-Haar 0.9413 0.0587	OPT-Haar HM
AVG	0.0639	18.0488	0.0703	0.0566	16.7590	0.0639
Local C	0.7443	0.9113	0.9050	0.7060	0.8437	0.8305
STD 2	0.2940	74.7509	0.2953	0.3358	78.0424	0.3137
Edge I	0.6325	172.0838	0.6778	0.5467	161.2350	0.6265
Entropy	7.7377	7.7413	7.7589	7.3122	7.4048	7.5996
PSNR	60.6781	6.1796	66.7422	62.7272	6.1041	67.3189
Q^{ab/f}	0.4746	0.0011	0.2795	0.3074	5.99*10 ⁻⁴	0.2230
Visual inspection						

are very important in many image processing applications and improving the entropy values indicating much detail information contained in the fused image. This approach makes a good use of the histogram matching and MCFO optimization techniques for providing better image quality, better visualization, and increasing the clearness of the fused images for accurate diagnosis and optimal therapy.

9 Conclusions

This paper provided an optimum solution for improving the performance of DWT fusion with different wavelet families (Haar, db1, Coiflet 1, discrete meyer), and PCA fusion

**Fig. 13** The effect of histogram matching on the PSNR values of the proposed MCFO-optimized wavelet-based fusion algorithm with Haar filter with different cases

techniques. The proposed strategy is based on the MCFO optimization technique which gives the optimum gain parameter values and the adaptive histogram equalization for improving the image quality and visualization. Different quality metrics are calculated to test and evaluate the proposed fusion algorithm to validate its effectiveness. Different realistic datasets have been tested with the proposed algorithm to confirm the efficiency and applicability to different medical modalities and diseases. The proposed MCFO-optimized wavelet-based fusion algorithm using Haar filter showed and achieved a superior performance compared to those of other wavelet filters, PCA, and traditional techniques using maximum fusion rule. It improves the values of average gradient, local contrast, edge intensity, and standard deviation, which indicates much more detailed information for better visualization. The processing time of the proposed algorithm ranges from 0.8 to 1.4 seconds, which is suitable for real-time applications. Finally, an investigation of the effect of histogram matching has been introduced for more enhancement of the image quality revealing higher PSNR, entropy, local contrast, and quality factor and producing very clear images with better visualization for accurate diagnosis.

References

1. Abdul-Ameer I, J Tan, Z Hou (2014) "Adaptive PCA-SIFT Matching Approach for Face Recognition Application", International Multi-Conference of Engineers and Computer Scientists IMECS, Vol 1, March 12–14, Hong Kong
2. Arunvinodh C, Davis AM (2015) "Comparative Analysis of Transform-Based Image Fusion Techniques for Medical Applications", IEEE Int. Conf. on Innovations in Information, Embedded and communication systems (ICIIECS). 1–6
3. Bick M (2015) "Central Force Optimization - Analysis of Data Structures & Multiplicity Factor", Master Thesis, University of Toledo, December
4. Daniel E, Anitha J, Kamaleshwaran KK, Rani I (2017) Optimum spectrum mask based medical image fusion using GrayWolf optimization. Biomed Sign Proc Control:36–43
5. Deserno TM (2011) "Fundamentals of Biomedical Image Processing", Biological and Medical Physics, Biomedical Engineering, DOI: https://doi.org/10.1007/978-3-642-15816-2_1, Springer Verlag Berlin Heidelberg
6. Donia EA, E-SM EL-Rabaie, GhM El-Banby, OS Faragallah, FE Abd El-Samie (2016) Infrared Image Enhancement Based on Both Histogram Matching And Wavelet Fusion, Fourth International Japan-Egypt Conference on Electronics, Communications and Computers (JEC-ECC). 111–114
7. Jagalingam P, Hegde AV (2015) A review of quality metrics for fused image. Aqua Proc 4:133–142
8. James AP, Dasarthy BV (2014) Medical image fusion: a survey of the state of the art. Inform Fus 19:4–19
9. Joseph J, Barhatte A (2014) "Medical Image Fusion Based on Wavelet Transform and Fast Curvelet Transform", IJEDR, Vol. 2, No. 1
10. Kannan K., Perumal S.A., Arulmozhi K. (2007) "Optimal Decomposition Level of Discrete Wavelet Transform for Pixel Based Fusion of Multi-Focused Images", International Conference on Computational Intelligence and Multimedia Applications. 314–318
11. Lee DTL, Yamamoto A (1994) "Wavelet Analysis: Theory and Applications", Hewlett-Packard Journal
12. Leng L, Zhang J, Xu J, Khan K, Alghathbar K (2010) "Dynamic Weighted Discrimination Power Analysis in DCT Domain for Face and Palmprint Recognition", [International Conference on Information and Communication Technology Convergence \(ICTC\)](#), Jeju, South Korea, 17–19
13. Leng L, J Zhang, G Chen, MK Khan, K Alghathbar (2011) "Two-Directional Two-Dimensional Random Projection and Its Variations for Face and Palmprint Recognition", International Conference on Computational Science and Its Applications. 458–470

14. Leng L, J Zhang, G Chen, K Khan, P Bai (2011) "Two Dimensional PalmPhasor Enhanced by Multi-orientation Score Level Fusion", International Conference on Secure and Trust Computing, Data Management, and Application, pp. 122–129
15. Leng L, S Zhang, X Bi, MK Khan (2012) "Two-Dimensional Cancelable Biometric Scheme", International Conference on Wavelet Analysis and Pattern Recognition, Xian, China
16. Leng L, M Li, L Leng, ABJ Teoh (2013) "Conjugate 2DPalmHash Code for Secure Palm-Print-Vein Verification", [6th International Congress on Image and Signal Processing \(CISP\)](#), Hangzhou, China, 16–18
17. Leng L, Li M, Kim C, Bi X (January 2017) Dual-source discrimination power analysis for multi-instance contactless Palmprint recognition. *Multimed Tools Appl* 76(1):333–354
18. Li S, Yang B, Hu J (2011) Performance comparison of different multi-resolution transforms for image fusion. *Inform Fus* 12(2):74–84
19. Liu Y, Nie L, Han L, Zhang L, Rosenblum DS (2015) "Action2Activity: Recognizing Complex Activities from Sensor Data", *IJCAI'15 Proceedings of the 24th International Conference on Artificial Intelligence*. 1617–162
20. Liu Y, Nie L, Liu L, Rosenblum DS (2016) From action to activity: sensor-based activity recognition. *Neurocomputing* 181:108–115
21. Mahmoud KR (2016) Synthesis of unequally-spaced linear array using modified central force optimisation algorithm. *IET Microw, Anten Propagation* 10(10):1011–1021
22. Mani VRS, Rivazhagan S (2013) "Survey of Medical Image Registration", *Journal of Biomedical Engineering and Technology*. 8–25
23. Mitchell HB (2010) "Image Fusion: Theories, Techniques and Applications", ISBN 978–3–642-11215-7, Springer-Verlag Berlin Heidelberg
24. Nabil A, Taha TE, Faragallah OS (2014) "Study of Advanced Fusion Methods in Medical Image Processing", M. Sc. Thesis, Faculty of Electronic Engineering, Menoufia University
25. Omar Z, Stathaki T (2014) "Image Fusion: An Overview", *International Conference on Intelligent Systems, Modelling and Simulation*
26. Rajini KC, Roopa S (2017) "A Review on Recent Improved Image Fusion Techniques", *IEEE Int. Conf. on Wireless Communications, Signal Processing and Networking*. 149–153
27. Raut GN, PL Paikrao, D S Chaudhari (2013) A Study of Quality Assessment Techniques for Fused Images. *IJITEE* 2, No. 4
28. Shahdoosti HR, Ghassemian H (2015) "Combining the Spectral PCA and Spatial PCA Fusion Methods by an Optimal Filter" *Tarbiat Modares University*
29. Patne G, Ghonge P, Tuckley K (2017) Review of CT and PET Image Fusion Using Hybrid Algorithm. *I2C2*
30. Song H, Qiu P (2017) Intensity-based 3D local image registration. *Pattern Recogn Lett* 94:15–21
31. Wang A, Sun H, Guan Y (2006) "The Application of Wavelet Transform to Multi-Modality Medical Image Fusion", *IEEE International Conference on Networking, Sensing and Control*. 270–274

Publisher's note Springer Nature remains neutral with regard to jurisdictional claims in published maps and institutional affiliations.



Heba M. El-Hoseny had the Ph. D. degree in Electronics and Electrical Communications Engineering from Benha University. Her areas of interest include medical image processing, and image encryption.



Zeinab Z. El Kareh Master Student in Industrial Electronics and Control Engineering Department, Faculty of Electronic Engineering, Menoufia University. Her areas of interest include medical image enhancement and fusion.



Wael A. Mohamed has got his Ph. D. from Cairo University, 2009. Now he is an Assistant Professor in Faculty of Engineering, Benha University. His areas of interest include digital signal and image processing.



Ghada M. El Banby received the M.Sc. and Ph.D. degrees in Automatic Control Engineering from Menoufia University, Egypt in 2006, and 2012, respectively. She works as a lecturer at the Department of Industrial Electronics and Control Engineering, Faculty of Electronic Engineering, Menoufia University. Her current research interests include computer vision, data fusion, systems, image processing, signal processing, medical imaging, modeling, and control.



Korany R. Mahmoud received his B.S. and M.S. degrees in Communications and Electronics Engineering from Helwan University in 1998 and 2003. His Ph.D. degree from Helwan University in collaboration with the University of Connecticut, USA in 2008. He is currently an associate professor at the department of communications and electronics engineering in the same faculty. Since 2012, Dr. Mahmoud served as a Consultant in the R&D department, National Telecommunications Regulatory Authority (NTRA), Egypt. Also, he has been working as a Post-Doctoral Fellow at the CPSM Center (Center for Photonics and Smart Materials), Zewail City, Egypt. His current research interests include the areas of 5G mm-Wave and optical antennas design, optimization techniques.



Osama S. Faragallah received the B.Sc. (Honors), M.Sc., and Ph.D. degrees in Computer Science and Engineering from Menoufia University, Menouf, Egypt, in 1997, 2002, and 2007, respectively. He is currently a Professor with the Department of Computer Science and Engineering, Faculty of Electronic Engineering, Menoufia University, where he was a Demonstrator from 1997 to 2002 and has been Assistant Lecturer from 2002 to 2007 and since 2007 he has been a Teaching Staff Member with the Department of Computer Science and Engineering, Faculty of Electronic Engineering, Menoufia University. He is a coauthor of about 150 papers in international journals and conference proceedings, and two textbooks. His current research interests include network security, cryptography, Internet security, multimedia security, image encryption, watermarking, steganography, data hiding, medical image processing, and chaos theory.



S. El-Rabaie (SM'92) was born in Sires Elian, Egypt, in 1953. He received the B.Sc. degree (with honors) in radio communications from Tanta University, Tanta, Egypt, in 1976, the M.Sc. degree in communication systems from Menoufia University, Menouf, Egypt, in 1981, and the Ph.D. degree in microwave device engineering from Queen's University of Belfast, Belfast, U.K., in 1986. In his doctoral research, he constructed a Computer-Aided Design (CAD) package used in nonlinear circuit simulations based on the harmonic balance techniques. Up to February 1989, he was a Postdoctoral Fellow with the Department of Electronic Engineering, Queen's University of Belfast. He was invited as a Research Fellow in the College of Engineering and Technology, Northern Arizona University, Flagstaff, in 1992 and as a Visiting Professor at Ecole Polytechnique de Montreal, Montreal, QC, Canada, in 1994. He has authored and co-authored more than 300 papers and nineteen textbooks. He was given several awards (Salah Amer Award of Electronics in 1993, The Best Researcher on (CAD) from Menoufia University in 1995). He acts as a reviewer and member of the editorial board for several scientific journals. He has participated in translating the first part of the Arabic Encyclopedia. Professor El-Rabaie was the Head of the Electronics and Communication Engineering Department, Faculty of Electronic Engineering, Menoufia University, and after that the Vice Dean of Postgraduate Studies and Research at the same Faculty. Prof. El-Rabaie is involved now in different research areas including CAD of nonlinear microwave circuits, nanotechnology, digital communication systems, biomedical signal processing, acoustics, antennas, and digital image processing. Now he is reviewer for the Quality Assurance and Accreditation of Egyptian for Higher Education. E-mail: srabie1@yahoo.com, Mobile:0020128498170.



Essam El-Madbouly received the B.Sc., in Nuclear Engineering, University of Alexandria, Egypt. He received PhD, in Electric Engineering, September 1983 University GH-Duisburg, Federal Republic of Germany. He is a Professor Emeritus of Industrial Electronics & Control, Faculty of Electronic Engineering, Menoufia University, Egypt. Professor Essam was a Member in Permanent Scientific Committee for Computer and automatic Control. He was a Consultant in Lord Precision Industry, Alexandria, Egypt. He was Research Fellowship from German Academic Service Exchange (DAAD), Department of Electrical Engineering (Communication) (Fachbereich Elektrotechnik, Nachrichtentechnik (Fachgebiet Mess- und Regelungstechnik)), University -GH-Duisburg, Federal Republic of Germany, from April 1978 to November 1983. Prof. Essam was Post Doctor Fellowship from DAAD in Germany in 1988. He worked an Engineer in atomic energy authority, Anshas, Egypt, 1969. He is involved in Supervision and

Discussion of several M.Sc. and PhD degrees in Faculties of Engineering (Menouf, Alexandria, Arab Academy for Science & Technology).



Fathi E. Abd El-Samie received the B.Sc., (Hons.), M.Sc., and Ph.D. degrees from Menuofia University, Menouf, Egypt, in 1998, 2001, and 2005, respectively. Since 2005, he has been a Teaching Staff Member with the Department of Electronics and Electrical Communications, Faculty of Electronic Engineering, Menoufia University. He was a researcher at KACST-TIC in Radio Frequency and Photonics for the e-Society (RFTONICS). His current research interests include image enhancement, image restoration, image interpolation, super-resolution reconstruction of images, data hiding, multimedia communications, medical image processing, optical signal processing, and digital communications. He was a recipient of the Most Cited Paper Award from the Digital Signal Processing journal in 2008.

Affiliations

Heba M. El-Hoseny¹ • Zeinab Z. El Kareh² • Wael A. Mohamed¹ • Ghada M. El Banby² • Korany R. Mahmoud³ • Osama S. Faragallah^{4,5} • S. El-Rabaie⁶ • Essam El-Madbouly² • Fathi E. Abd El-Samie⁶

¹ Department of Electrical Engineering, Faculty of Engineering, Benha University, Benha, Egypt

² Department of Industrial Electronics and Control Engineering, Faculty of Electronic Engineering, Menoufia University, Menouf, Egypt

³ Department of Electronics, Communications, and Computers, Faculty of Engineering, Helwan University, Cairo, Egypt

⁴ Department of Computer Science and Engineering, Faculty of Electronic Engineering, Menoufia University, Menouf 32952, Egypt

⁵ Department of Electronics and Electrical Communications Engineering, Faculty of Electronic Engineering, Menoufia University, Menouf 32952, Egypt

⁶ Department of Information Technology, College of Computers and Information Technology, Taif University, Al-Hawiya 21974, Saudi Arabia